

Lecture 7: Stress Relaxation

E. J. Hinch

1 Introduction

How does a Non-Newtonian fluid behave when under stress? And what happens when the force causing the stress is removed? One would expect that purely elastic solids when combined with viscous fluids would be adequate in modeling Non-Newtonian fluids. However, that is not the case.

As is apparent in figure 1, there is a certain time scale characteristic of Non-Newtonian fluids that is absent when such substances are modeled as a mix of elastic solids and viscous fluids. Accounting for a *relaxation time* of the microstructure and the extra normal stresses is essential to the description of such materials.

When a Non-Newtonian fluid is deformed, the instantaneous viscous stress that builds up scales as $\mu_o \dot{\gamma}$, where μ_o is the zero-shear viscosity of the material. If we now suppose that there is a memory time (τ) associated with the microstructure within the material, then the deformation it undergoes for a constant shear rate, $\dot{\gamma}$, would be $\dot{\gamma}\tau$. As in elastic solids, the elastic stress associated with such a deformation would be $G\dot{\gamma}\tau$, where G is the elastic modulus of the material. After the memory time or the relaxation time of the material has elapsed, the stress would reach a steady value which would scale as $(\mu_o + G\tau)\dot{\gamma}$ as seen in figure 1. It is reasonable to think of $(\mu_o + G\tau)$ as an enhanced viscosity. In other words, Non-Newtonian fluids have a characteristic memory time scale which is referred to as the *relaxation time*. When the applied rate of deformation is reduced to zero, these materials relax over their characteristic relaxation time - a constitutive property of each material. This phenomenon is known as stress relaxation.

2 Flow of a non-Newtonian fluid past a rigid sphere

We will now look at the flow of a Non-Newtonian fluid past a sphere. While such a flow can be steady in an Eulerian sense, it might be unsteady in a Lagrangian sense. Arigo *et al*, [1] worked out the FEM simulations of the long wake behind the sphere using the Oldroyd-B model for the microstructure, as shown in figure 2. Note that the wake gets longer as the Deborah number, De , increases. This is because as the shear rate is increased, the fluid behind the wake is stretched more and more, therefore requiring a larger distance to relax.

In figure 3, the force required to move the sphere at a constant velocity through the fluid is plotted against Weissenberg number (which for this case may be thought of as the dimensionless shear rate). The force is made dimensionless with the equivalent Stokes

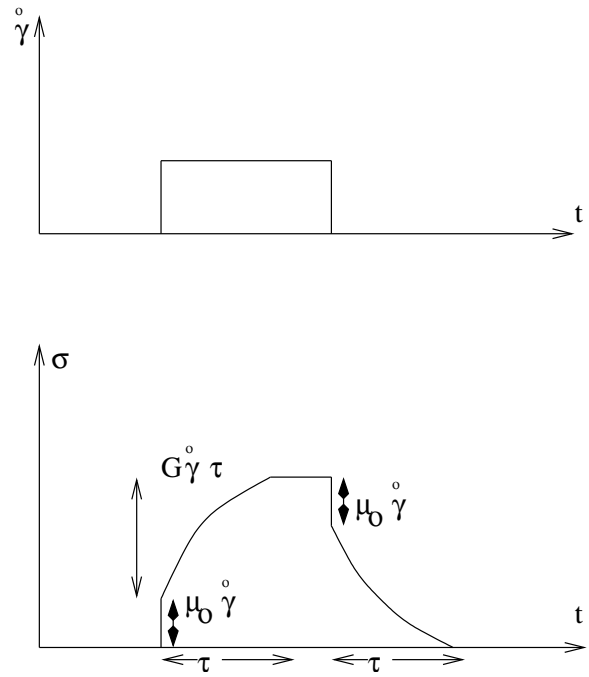


Figure 1: Stress build-up and relaxation in a viscoelastic material due to a step strain rate.

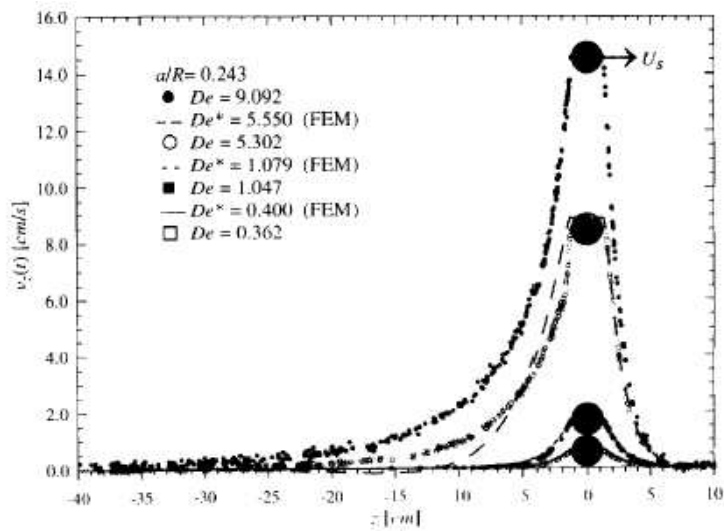


Figure 2: Velocity in the wake of a rigid sphere moving through a non-Newtonian fluid, as a function of the distance from the center of the sphere.

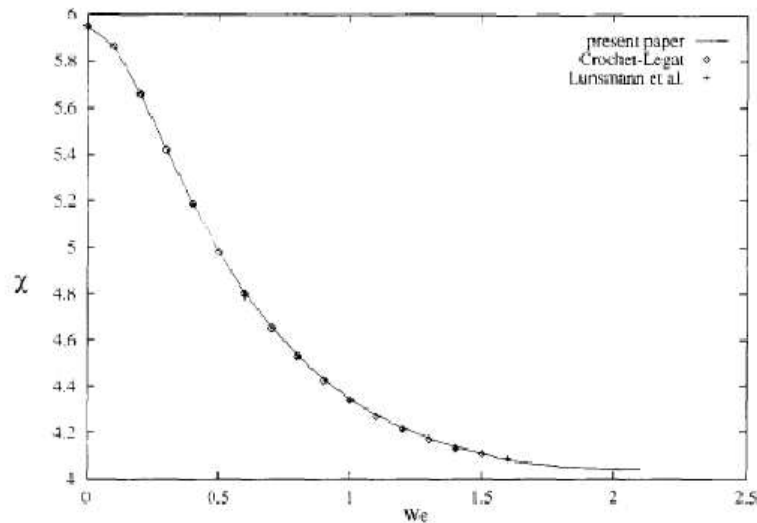


Figure 3: Drag on the sphere, scaled with Stokes drag, plotted against the Weissenberg number.

drag - the force that would have been required to move the sphere at the same velocity in a Newtonian fluid of viscosity $(\mu_o + G\tau)$ [2]. A comparison with the experiments shows that the force required does not decrease as drastically as predicted by the Oldroyd-B calculation [3], as shown in figure 4. The simulations can be brought closer to the experimental observation by calculating the Stokes drag using the zero-shear viscosity of the fluid instead of the deformation enhanced viscosity. This is because, as the sphere is moved faster (up to a limit), the fluid gets less time to deform. Hence the viscosity as seen by the sphere still remains μ_o . Two of the important experimental observations that the Oldroyd-B model fails to predict are the large increase in drag beyond a critical We and the much larger wake seen behind the sphere.

When a sphere moves through a Non-Newtonian fluid, negative wakes are observed. In a negative wake, the fluid in the wake region of a moving sphere starts to move in a direction opposite to that of the sphere. Figure 5 shows a cartoon describing the effect. These negative wakes have been ascribed to the high stresses that the moving sphere introduces in its wake regions as it deforms the microstructure. The stress relaxation of the fluid after the sphere has moved away from a point causes a secondary flow.

Another calculation was done by Harlen [4] using a finite extensible non-linear elastic (FENE-CR) microstructure model proposed by Chilcott and Rallison, a figure from which is shown in figure 6. This simulation demonstrates that the extent of negativity in a wake increases as the extensibility (parameter L in figure) of the microstructure increases.

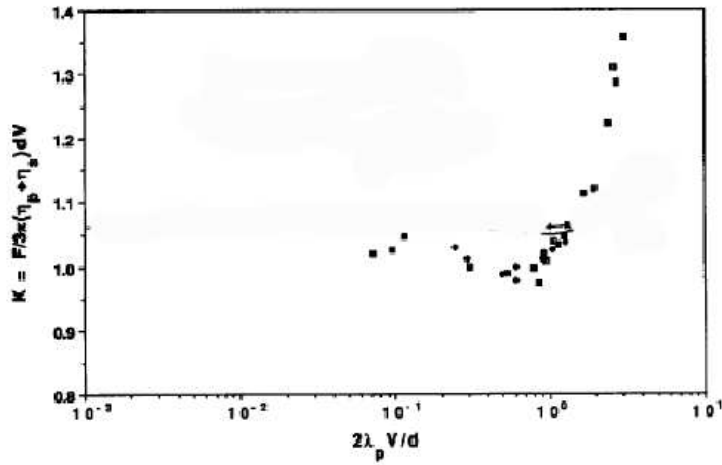


Figure 4: Drag on the sphere plotted against Weissenberg number, measured experimentally.

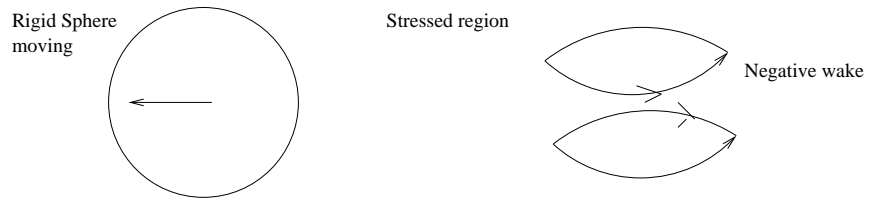


Figure 5: Cartoon showing a negative wake region behind the sphere

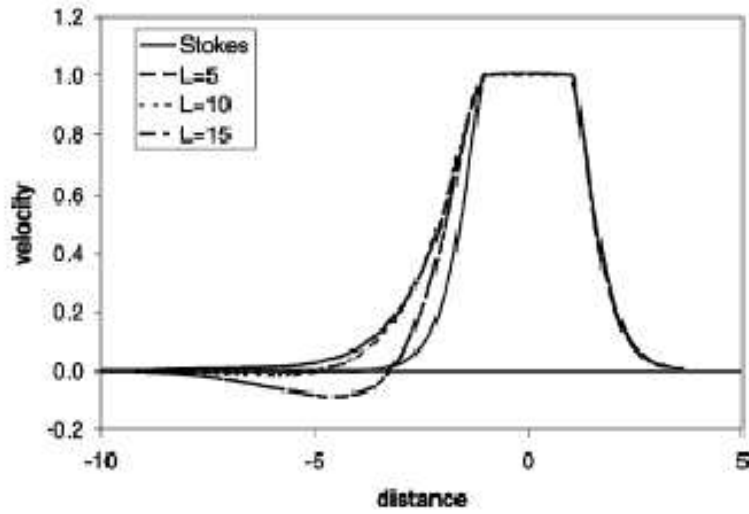


Figure 6: The negative wake as seen in FENE-CR calculations.

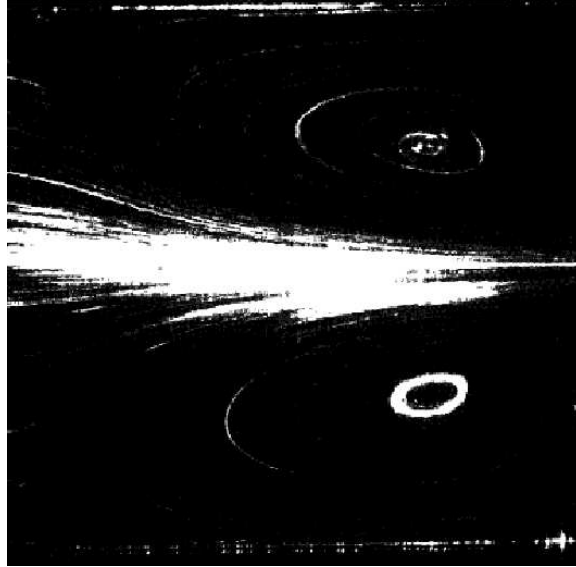


Figure 7: A picture from an experiment, showing the upstream vortex in the contraction flow of a non-Newtonian fluid.

3 Flow of a non-Newtonian fluid through a sudden contraction

Large upstream vortices are observed in Non-Newtonian fluids flowing through a channel contraction as shown by Cartalos and Piau [5] (see figure 7). This is another example of a flow which may be unsteady in the Lagrangian sense while being steady in the Eulerian sense. Oldroyd-B model has been used in the FEM simulations of such flows ([6, 7]). In figure 8, we can see the pressure drop (made dimensionless with the Stokes drag) across the contraction plotted against the Deborah number. This result disagrees with what is observed in experiments (see figure 9) wherein an initial decrease in the pressure drop is followed by a steady climb up to an order of magnitude higher value. Thus Oldroyd-B successfully predicts the initial small decrease in pressure drop until a De of about 5. However, it fails to predict the large upstream vortices and the dramatic increase in pressure drop seen in constraction flows of such fluids. Again, it is better to scale the pressure drop for higher De using μ_o instead of $(\mu_o + G\tau)$ as explained for a sphere moving in a Non-Newtonian fluid.

Arigo, *et al.* [1] worked out the FEM simulation of a sphere falling down a tube filled with a Non-Newtonian fluid, wherein a constant force was applied to move the sphere. Figure 10 shows the velocity of the sphere as it descends down the tube. Again, Oldroyd-B is the model that has been used in the calculation. In the figure, it is evident that the velocity of the sphere overshoots the Newtonian value during start-up of the fall. This is due to shear-thinning. After reaching a peak, the velocity begins to decrease and becomes less than the Newtonian case after a sufficiently long time. Increasing the Deborah number results in the sphere slowing down more quickly.

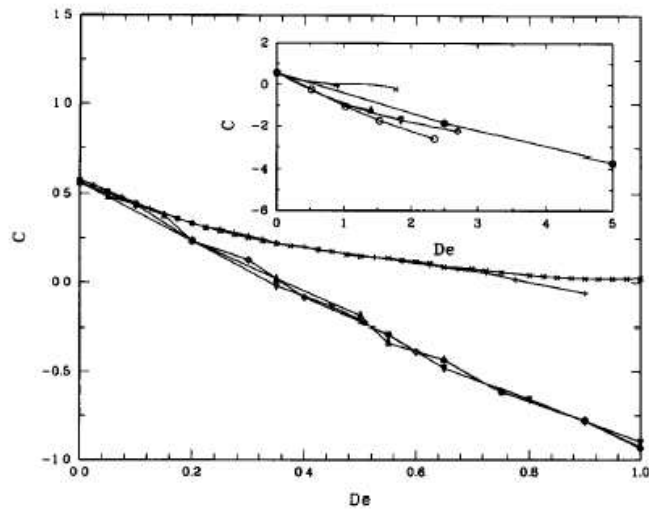


Figure 8: Pressure drop across the contraction, calculated using the Oldroyd-B model, plotted against De .

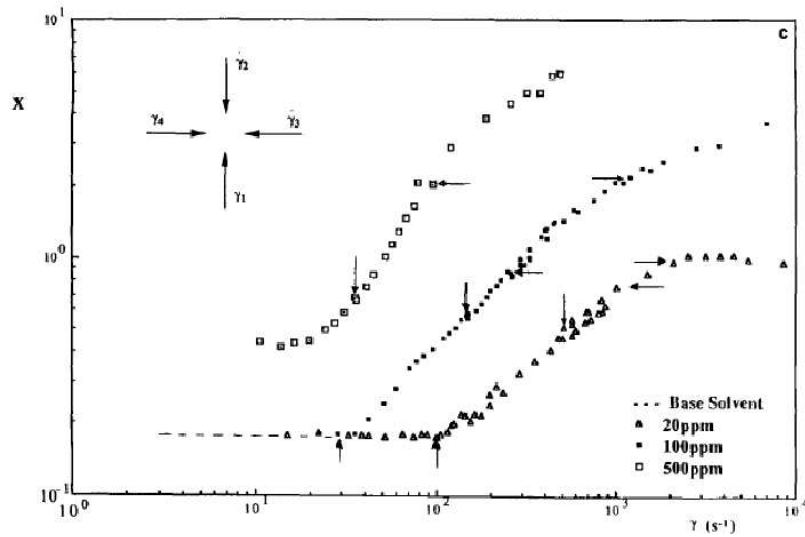


Figure 9: Experimental results of pressure drop in a contraction flow plotted against strain rate.

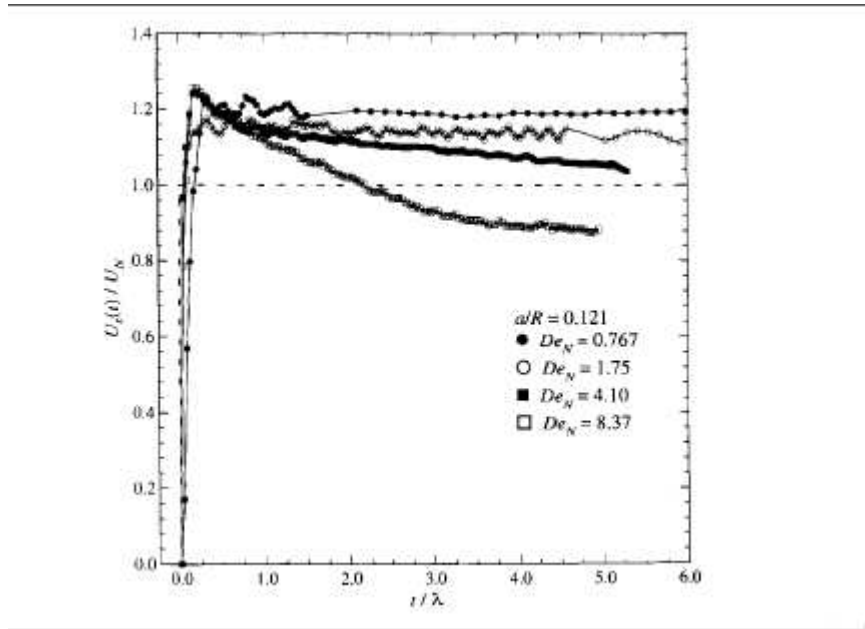


Figure 10: Velocity of the sphere plotted against time

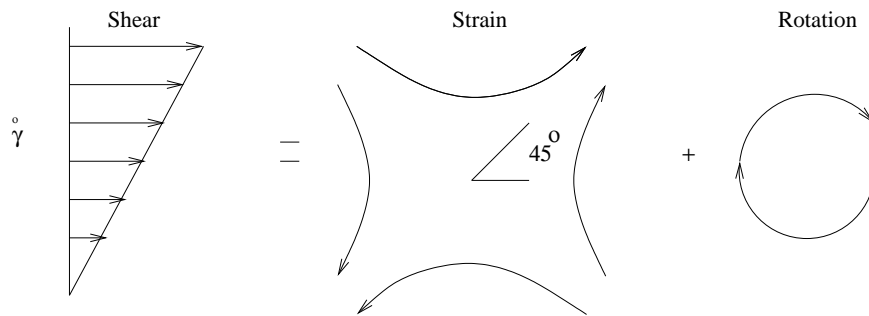


Figure 11: Shear flow can be written as a sum of straining and rotation.

3.1 Non-linear deformation

When a Non-Newtonian fluid undergoes a nonlinear deformation, tension in the streamlines develops due to the large relaxation time of the microstructure. This tension in the streamlines results in non-zero normal stresses within the fluid. We can estimate the approximate shear and normal stresses in Non-Newtonian fluid deformed by a simple shear flow in the following manner. The simple shear flow can be decomposed into a purely straining motion with the principal axes oriented at 45° from the axis of shear and a pure rotation as is shown in figure 11.

The straining motion causes a strain of $\dot{\gamma}\tau$ resulting in a shear stress equal to $G\dot{\gamma}\tau$ in the microstructure. Pure rotation then causes the microstructure to align in the direction of the flow, thereby lending it to compression by the straining motion, as shown in figure

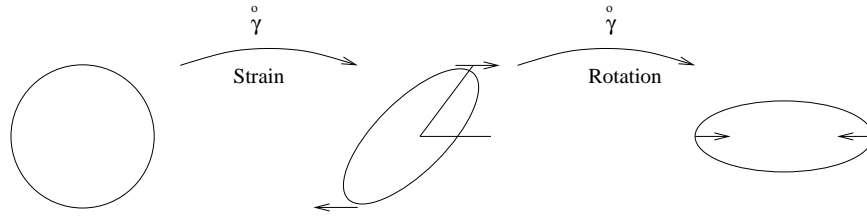


Figure 12: Shear and Normal Stresses in a non-Newtonian fluid.

12. The extent of the compression is $\dot{\gamma}\tau$. Thus

$$\text{Normal Stress} = \text{Shear Stress} \times \dot{\gamma}\tau$$

4 Yield Problems

Some Non-Newtonian fluids undergo a yield behavior when deformed beyond a limit. Such fluids have an associated yield stress beyond which it undergoes a distinct change in flow behavior. Common examples of materials that possess a yield stress are foams, cross-linked gels and pastes. In this lecture we will talk about such materials and then describe some of the common applications of yielding in the transport of small particles as well as the dangers of having a dead zone in sharp corners of channels. We will then proceed to the age-old squeeze film paradox. After that we will talk about what is common between ketchup bottles and oil pipelines.

Kabla & Debregeas [8] has suggested that foams get permanently damaged upon yielding. Therefore, an understanding of the yield behavior of foams is of direct relevance to their efficacy. The figure 13 has been taken from St.Jalmes & Durian [9]. They show how the yielding stress and strain decrease with decreasing volume fraction of gas in a foam. The rheological behavior of an unnamed cross-linked gel is shown in figure ???. Both the degree of cross-linking and the concentration of the polymer molecules forming the gel will determine its yield stress.

Yield stress is an important quantity when walls are being plastered. If the yield stress of the plaster is too large, it will not flow very smoothly - sticking, slipping and bringing into question the self-esteem of the painter. However, if the yield stress is too small, painting the ceiling will be an exercise in making the floor dirty because all the plaster paste will give in to gravity. The figure ??? shows the yielding behavior of a suspension of 30% Aluminium particles in an unknown solvent. Clearly, the yielding behavior is strongly governed by the pH of the suspension. An explanation for this is still lacking.

Another interesting effect of yield stress can be seen in the sedimentation of rigid particles in a Bingham fluid. In order for the particle to sediment, the stress due to gravitational force should be higher than the yield stress of the fluid. When that happens, a fluid region is created around the particle that will cause it to cruise through the Bingham fluid and sediment, as can be seen in figure 14. For the case of a spherical particle, there are two stagnation points where the stress is below yield stress. Hence, they remain undeformed and can be treated as solid regions. Detailed calculations for this problem can be found in work by Beris *et al* [10].

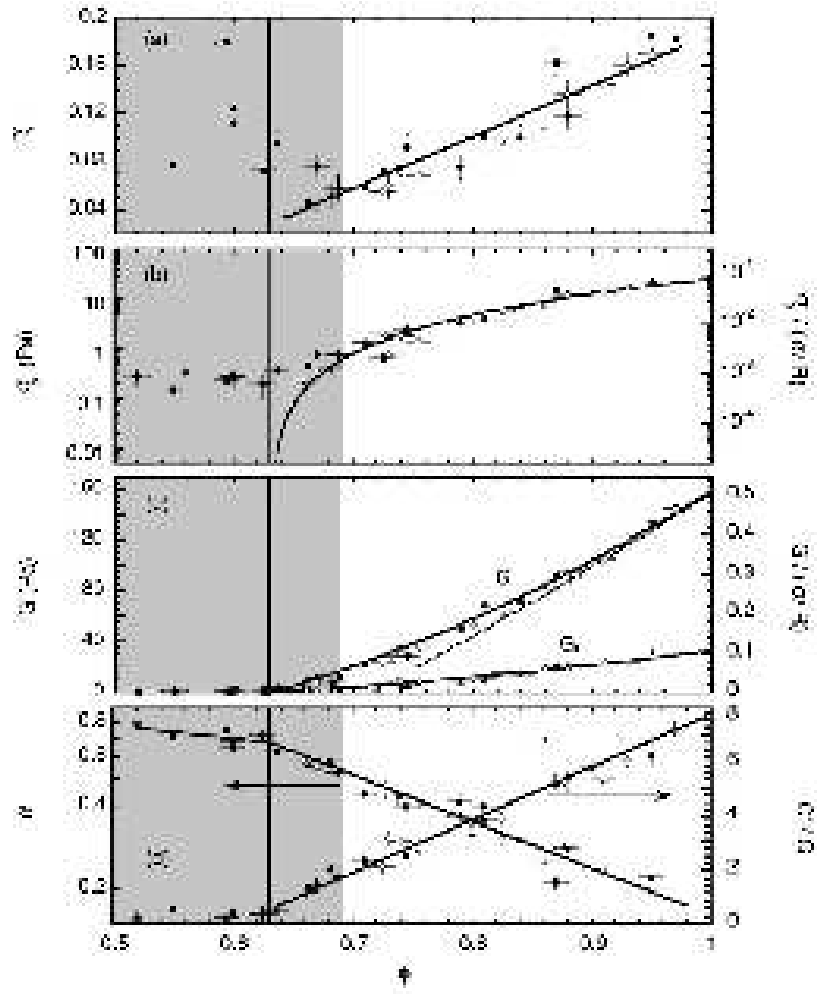


Figure 13: Yield strain and yield stress of a foam Vs. volume fraction of gas.

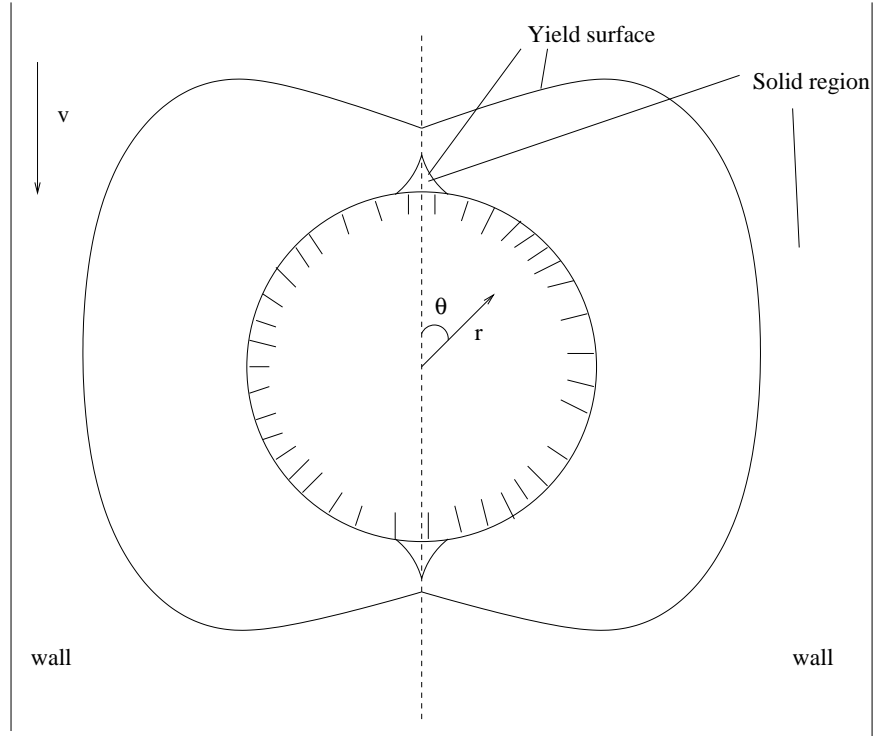


Figure 14: Sedimentation of a sphere in a Bingham fluid.

When a Bingham yield fluid flows through a rectangular channel, the fluid near the corner can remain unyielded as seen in figure 15.

5 Squeeze film paradox

In this section, we will talk about the squeeze film paradox. First, we will describe this paradox. After that, we will address the solution of this problem [11, 12, 13].

As shown in Fig. 16, we consider a film of Bingham fluid described in terms of a Cartesian coordinate system (x, z) in which x is the horizontal and z the vertical. Let the center of the film lie at the origin. If we squeeze the film with the vertical velocity $W/2$ from above and the vertical velocity $-W/2$ from below, the film will move horizontally with the velocity u and vertically with the velocity w (Shown in figure 16). If the effect of gravity is ignored, the momentum equations for the film are:

$$0 = -\frac{\partial p}{\partial x} + \sigma_{xx,x} + \sigma_{xz,z}, \quad (1)$$

$$0 = -\frac{\partial p}{\partial z} + \sigma_{xz,x} + \sigma_{zz,z}. \quad (2)$$

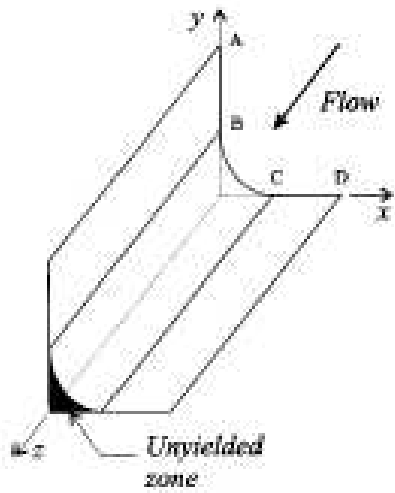


Figure 15: Unyielded zone in the corner of a rectangular channel.

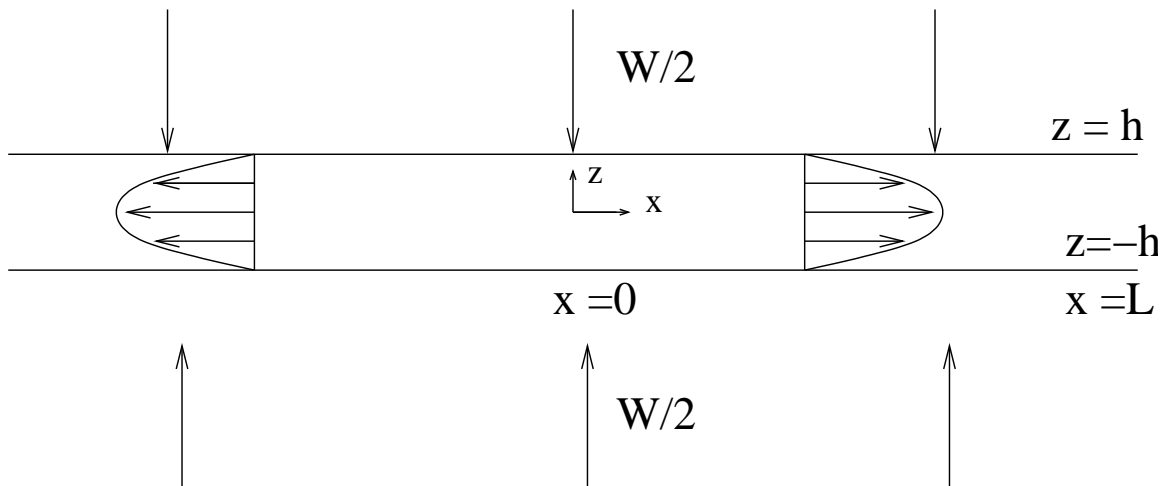


Figure 16: Squeezing of the film

For a Bingham fluid, the relationship between the stress and strain rate is

$$\mathbf{E} = \mathbf{0} \quad \text{if } |\sigma| < \sigma_y, \quad (3)$$

$$\sigma = \left(2\mu + \frac{\sigma_y}{|\mathbf{E}|}\right)\mathbf{E} \quad \text{if } |\sigma| > \sigma_y, \quad (4)$$

where σ_y is the yield stress, \mathbf{E} is the strain rate tensor and σ is the stress tensor. \mathbf{E} can be expressed as:

$$\mathbf{E} = \begin{pmatrix} u_x & \frac{1}{2}(u_z + w_x) \\ \frac{1}{2}(u_z + w_x) & w_z \end{pmatrix}. \quad (5)$$

The second invariant of the strain rate tensor and the stress tensor are: $|\mathbf{E}| = \sqrt{\frac{1}{2}\mathbf{E} : \mathbf{E}}$ and $|\sigma| = \sqrt{\frac{1}{2}\sigma : \sigma}$ respectively. We non-dimensionalize the momentum equation in the following way. Let L be the horizontal length scale, H be the vertical length scale, and W be the scale for the vertical velocity. Then the horizontal velocity u can be scaled as $W \frac{L}{H}$, and strain rate tensor E can be scaled as $\frac{W}{L}$. Also we scale σ_y, σ_{xz} by $\frac{\mu WL}{H^2}$ and σ_{xx}, σ_{zz} by $\frac{\mu W}{H}$, and the pressure p by $\frac{\mu WL^2}{H^2}$. Let $\epsilon = \frac{H}{L}$. Since the horizontal length scale L is much larger than the vertical length scale H , we have $\epsilon \ll 1$, $p \gg (\sigma_y, \sigma_{xz}) \gg (\sigma_{xx}, \sigma_{zz})$. Then the non-dimensionalized equation can be written as:

$$0 = -\frac{\partial p}{\partial x} + \epsilon^2 \sigma_{xx,x} + \sigma_{xz,z}, \quad (6)$$

$$0 = -\frac{1}{\epsilon^2} \frac{\partial p}{\partial z} + \sigma_{xz,x} + \sigma_{zz,z}. \quad (7)$$

To $O(\epsilon^2)$, the momentum equation in the z direction is:

$$\frac{\partial p}{\partial z} = 0. \quad (8)$$

Thus, the pressure is not a function of the height to $O(\epsilon^2)$:

$$p = p(x) + O(\epsilon^2). \quad (9)$$

The non-dimensionalized strain rates are:

$$\mathbf{E} = \begin{pmatrix} \epsilon u_x & \frac{1}{2}(u_z + \epsilon^2 w_x) \\ \frac{1}{2}(u_z + \epsilon^2 w_x) & \epsilon w_z \end{pmatrix}. \quad (10)$$

So the leading order constitutive law will be:

$$u_z = 0 \quad \text{if } |\sigma_{xz}| < \sigma_y, \quad (11)$$

$$\sigma_{xz} = -\sigma_y + \dot{\gamma} u_z \quad (\text{in } z > 0) \quad \text{if } |\sigma_{xz}| < \sigma_y, \quad (12)$$

$$\sigma_{xz} = +\sigma_y - \dot{\gamma} u_z \quad (\text{in } z < 0) \quad \text{if } |\sigma_{xz}| < \sigma_y. \quad (13)$$

Integrating the momentum equation along the x-direction with respect to z , we find:

$$\sigma_{xz} = \frac{dp}{dx} z + O(\epsilon^2) \quad (14)$$

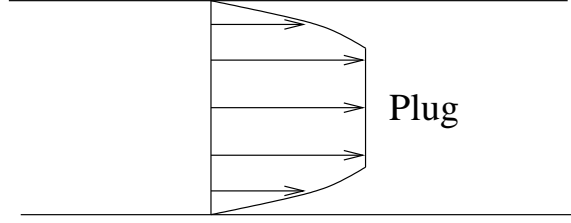


Figure 17: Plug velocity profile in the unyielded region of the film.

By introducing equation (14) into the leading order constitutive law equation(11-13) at the yielding level $z = Y$, we find that:

$$\frac{dp}{dx}Y = -\sigma_y. \quad (15)$$

Hence the yield level Y can be expressed as:

$$Y = \sigma_y / \left(-\frac{dp}{dx} \right). \quad (16)$$

The velocity gradient in the z -direction then becomes:

$$u_z = \begin{cases} 0 & \text{in } 0 \leq z \leq Y \\ \frac{dp}{dx}(z - Y) & \text{in } Y \leq z \leq 1. \end{cases} \quad (17)$$

Integrating in z , we obtain the velocity profile as:

$$u = \begin{cases} U & \text{in } 0 \leq z \leq Y \\ U + \frac{dp}{dx} \frac{1}{2}(z - Y)^2 & \text{in } Y \leq z \leq 1. \end{cases} \quad (18)$$

When the height z is less than the yield level Y , the fluid in the film will not yield and move with a uniform plug velocity U . When the height z is larger than the yield level Y , the velocity of the fluid in the film increases quadratically with height (See in figure 17).

Assume the non-slip boundary condition:

$$u = 0 \quad \text{at } z = 1. \quad (19)$$

Then match the velocity profile to the non-slip boundary condition; we have:

$$\frac{dp}{dx} = -\frac{2U}{(1 - Y)^2}. \quad (20)$$

Substituting the pressure gradient along the x direction into the velocity profile, we have

$$u = \begin{cases} U & \text{in } 0 \leq z \leq Y \\ U \left[1 - \frac{(z - Y)^2}{(1 - Y)^2} \right] & \text{in } Y \leq z \leq 1. \end{cases} \quad (21)$$

Therefore, we obtain the horizontal velocities of the film at different heights. However, that is not the end of the story. Integrating the horizontal velocity along the z direction, we can obtain the volume flux Q :

$$Q = \int_0^1 u dz = U \left[\frac{2}{3} + \frac{1}{3}Y \right]. \quad (22)$$

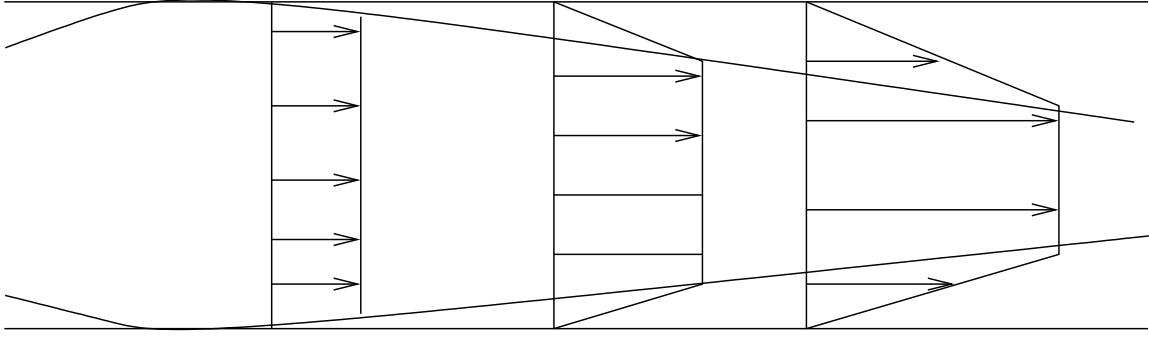


Figure 18: The velocity is increasing in the x direction – paradox!

As we squeeze the film, the sum of the horizontal flux Q of the fluid should be equal to the decrease of the fluid volume in the vertical direction per unit time because of the mass conservation:

$$Q = \frac{1}{2}x. \quad (23)$$

Combining the two equations above, we obtain the expression for the plug velocity U .

$$U = \frac{\frac{1}{2}x}{\frac{2}{3} + \frac{1}{3}Y}. \quad (24)$$

Putting this into the expression for the pressure gradient along the x -direction, we have:

$$\frac{dp}{dx} = -\frac{x}{\left(\frac{2}{3} + \frac{1}{3}Y\right)(1-Y)^2}. \quad (25)$$

After substituting the pressure gradient along the x direction into the expression for the yield level, we obtain an equation for the yield level Y :

$$Y = \sigma_y \left(\frac{2}{3} + \frac{1}{3}Y \right) (1-Y)^2/x. \quad (26)$$

The asymptotic solution of this equation is:

$$Y \sim \begin{cases} 1 - x^{\frac{1}{2}} & \text{in } x \ll 1 \\ \frac{2\sigma_y}{3x} & \text{in } x \gg 1. \end{cases} \quad (27)$$

By introducing the expression for the yield level Y into the equation for the plug velocity U , we find that the plug velocity U is not a constant any more, but varies in the horizontal direction x (See figure 18), which contradicts with the previous conclusion. This is known as the squeeze film paradox.

To resolve the squeeze film paradox, we show how plug velocity U can be a function of x if we assume the stress is actually just above the yield value in the “plug” region: $|\sigma| = \sigma_y + O(\epsilon)$. Now, the stress is given by,

$$\sigma_{xz} = -\sigma_y \frac{z}{Y}, \quad (28)$$

Thus $|\sigma| \approx \sigma_y$ if

$$\sigma_{xx} = -\sigma_{zz} = \sigma_y \sqrt{1 - \frac{z^2}{Y^2}} + O(\epsilon). \quad (29)$$

Since the strain rate tensor E is proportional to the stress tensor for the Bingham fluid, the derivative of the horizontal velocity u with respect to z should have first order approximation, $u_z = O(\epsilon)$, and we could assume that the horizontal velocity u can be expanded as $u = U(x) + \epsilon u_1(x, z)$. Then the strain rate tensor can be expressed as:

$$\mathbf{E} = \epsilon \begin{pmatrix} U_x & \frac{1}{2}u_{1z} \\ \frac{1}{2}u_{1z} & -U_x \end{pmatrix}. \quad (30)$$

Therefore the magnitude of the strain rate tensor is: $|\mathbf{E}| = \epsilon \sqrt{\mathbf{U}_x^2 + \frac{1}{4}\mathbf{u}_{1z}^2}$, and we have

$$-\sigma_y \frac{z}{Y} = \sigma_{xz} = \left(2 + \frac{\sigma_y}{\epsilon \sqrt{U_x^2 + \frac{1}{4}u_{1z}^2}} \right) \epsilon \frac{1}{2}u_{1z}. \quad (31)$$

Thus, u_{1z} satisfies:

$$u_{1z} = -\frac{2U_x \frac{z}{Y}}{\sqrt{1 - \left(\frac{z}{Y}\right)^2}}. \quad (32)$$

This solution is singular as z approaches the yielding level Y , requiring a thin transition layer of order $O(\epsilon)$, across which we must match the pseudoplug solution with the earlier solution for the yielding region in order to fully specify the flow. Without going through this refinement, we may still integrate equation (32) to find the velocity connection inside the plug,

$$u_1 = 2U_x Y \sqrt{1 - \left(\frac{z}{Y}\right)^2}. \quad (33)$$

Therefore, the horizontal velocity u varies in the x and the z directions even in the plug region as predicted.

6 Ketchup bottles and oil pipelines

There are great reservoirs underneath the ocean. In the petroleum industry, oil is often pumped through long pipelines to the sea surface. The length of the pipelines is usually 3 km, and the diameter of the pipelines is usually 10cm. When the oil is pumped up out of these reservoirs, the temperature of the oil is high ($\sim 80^\circ C$) and the viscosity of the oil is low. During transport, the cold water in the ocean ($\sim 4^\circ C$) cools the oil. To insulate the pipeline from the ocean water and ease pumping, insulating gel is put between the pipelines. A practical problem which then occurs is that the hot oil pipe will also heat the gel and make the gel expand. People usually build a vacant expansion pipe to contain the expanded gel. After the production stops, the oil pipe cools and gel contracts. The contracted gel is then

recycled. Three questions emerge that need to be answered before the production process: Will the gel convect with the large temperature difference $\Delta T = 80^\circ C$? Can we generate the pressure to pump the oil 3Km in 10 hours without bursting the pipe? How much gel flows out of the expansion pipe in the recycling process?

We address these questions one by one. First, let us consider whether the gel will convect. Before we answer this question, we need to calculate the yield stress of the gel. Lab observations show that a 1mm air bubble does not move in the vertical gel pipe and air bubbles larger than 1mm will move. A balance of buoyant stress and the yield stress of the gel(τ_*) gives the following estimate:

$$\tau_* = \Delta\rho_0gd = 10 \text{ Pa}, \quad (34)$$

where the $\Delta\rho_0$ is the density difference between the gel and air, and d is the diameter of the bubble. Therefore, the yield stress of the gel is about $10Pa$. Near the surface of the oil pipe the temperature of the gel is around $80^\circ C$, and the temperature of the gel near the cold water is around $4^\circ C$. The temperature difference between the cold gel and the hot gel will therefore be about: $\Delta T \sim 80^\circ C$. The density difference for the gel at these different temperatures is:

$$\frac{\Delta\rho}{\rho} = 10^{-2}. \quad (35)$$

Consequently, there will be a buoyant force on a “bubble” of the heated gel. From Eq. 34, a bubble of diameter D will be held in place by the yield stress if:

$$\tau_* \approx 10Pa > \Delta\rho gD = 10^{-2} \cdot 10 \cdot D, \quad (36)$$

that is, if $D < 10cm$. Since the diameter of the pipe is about 10cm, the gel will not convect.

Now, let us consider whether pumping is feasible. For pumping, the pressure difference across the pipe should exceed the yield stress of the gel along the wall:

$$\pi r^2 \Delta p > 2\pi r L \tau_*, \quad (37)$$

where r is the radius of the pipe, L is the length of the pipe, Δp is the pressure difference across the pipe, and τ_* is the yield stress of the gel. Therefore, we estimate pressure drop per unit length as:

$$\frac{\Delta p}{L} = 200Pa \cdot m^{-1}. \quad (38)$$

Measurement shows that the pressure drop per unit length in the oil pipes is $350Pam^{-1}$ in the 100m long pipe test. Therefore, the gel will flow. For the 3km long pipe, the total pressure drop will be: $\Delta p = 6bar$. Since the strength of the pipe is about 50bar, it is also safe for pumping gel to 3Km in 10 hours.

In the hot oil pipe, the gel expands and flows into the special expansion pipe. When the production stops, the pipe cools, and the gel contracts. Does the gel flow out of the expansion pipe? Before answering this question, let us look at a ketchup bottle problem and calculate how much fluid comes out of the ketchup bottle.

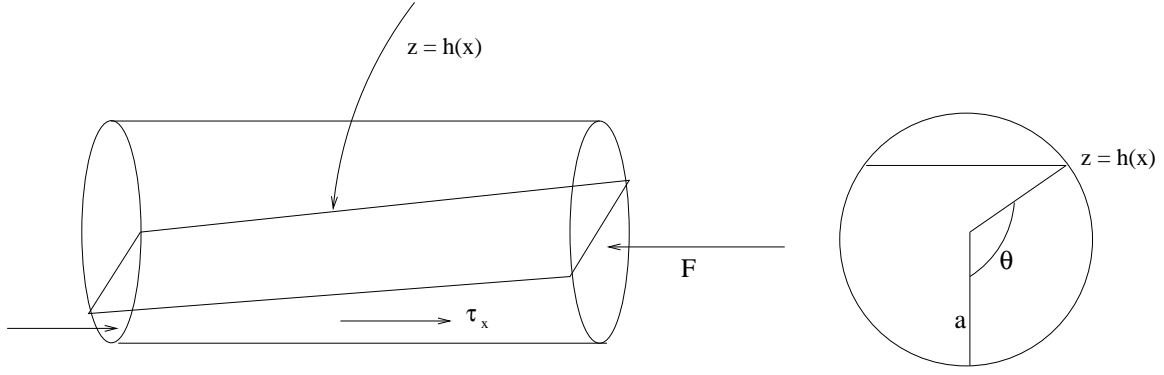


Figure 19: The flow of gel inside the expansion pipe is similar to that of ketchup in a bottle.

For an idealized cylindrical ketchup bottle, let x be the distance along the bottle, z be the height of the ketchup in the bottle $z = h(x)$, and A be the cross section of the ketchup in the bottle.

Then the pressure force is:

$$F = \int p dA, \quad (39)$$

where p is the hydrostatic pressure produced by the ketchup. Then the gradient of the pressure force along the x direction is:

$$\frac{dF}{dx} = \rho g \frac{dh}{dx} A. \quad (40)$$

In the steady state, the pressure gradient force is balanced by the friction between the ketchup and the wall of the ketchup bottle. The ketchup can flow if the friction stress is larger than the yield stress of the ketchup:

$$\rho g \frac{dh}{dx} A > \tau_* 2a\theta, \quad (41)$$

where τ_* is the yield stress and $2a\theta$ express the wetted area per unit length, with the angle θ defined as in figure 19. The height of the wetted area can be expressed as $h = a(1 - \cos(\theta))$ and $A = a^2(\theta - \frac{1}{2} \sin(\theta))$. Substituting these two expression into the equation of the pressure gradient force, we get

$$\frac{d\theta}{dx} > \frac{\tau_*}{\rho g a^2} \frac{2\theta}{\sin(\theta)(\theta - \frac{1}{2} \sin(\theta))}. \quad (42)$$

Therefore, flow will continue until the inequality becomes an equality, giving the volume removed from a ketchup bottle:

$$V = a^3 \frac{\rho g a}{\tau_*} 1.69, \quad (43)$$

from a length $a \frac{\rho g a}{\tau_*} 0.85$. This calculation fits well with experiments.

Notes by Junjun Liu and Anshuman Roy

References

- [1] M. T. Arigo, D. Rajagopalan, N. Shapley, and G. H. McKinley, "The sedimentation of a sphere through an elastic fluid. part 1. steady motion," *Journal of Non-Newtonian Fluid Mechanics* **60(2-3)**, 225 (1995).
- [2] F. Yuran and M. D. Crochet, "High-order finite element methods for viscoelastic flows," *Journal of Non-Newtonian Fluid Mechanics* **57(2-3)**, 283 (1995).
- [3] V. Tirtaadmadja, P. H. T. Uhlherr, and T. Sridhar, "Creeping motion of spheres in fluid m1," *Journal of Non-Newtonian Fluid Mechanics* **35(2-3)**, 327 (1990).
- [4] O. G. Harlen, "The negative wake behind a sphere sedimenting through a viscoelastic fluid," *Journal of Non-Newtonian Fluid Mechanics* **108(1-3)**, 411 (2002).
- [5] U. Cartalos and J. M. Piau, "Creeping flow regimes of low concentration polymer solutions in thick solvents through an orifice die," *Journal of Non-Newtonian Fluid Mechanics* **45(2)**, 231 (1992).
- [6] B. Debbaut, J. M. Marchal, and M. J. Crochet, "Numerical-simulation of highly viscoelastic flows through an abrupt contraction," *Journal of Non-Newtonian Fluid Mechanics* **29(1-3)**, 119 (1988).
- [7] P. J. Coates., R. C. Armstrong, and R. A. Brown, "Calculation of steady-state viscoelastic flow through axisymmetric contractions with the eeme formulation," *Journal of Non-Newtonian Fluid Mechanics* **108(1-3)**, 411 (1992).
- [8] A. Kabla and G. Debregeas, "Local stress relaxation and shear banding in a dry foam under shear," *Physical review letters* **90(25)**, Art. No. 258303 (2003).
- [9] A. Saint-Jalmes and D. J. Durian, "Vanishing elasticity for wet foams: Equivalence with emulsions and role of polydispersity," *Journal of Rheology* **43(6)**, 1411 (1999).
- [10] A. N. Beris, J. A. Tsamopoulos, R. C. Armstrong, and R. A. Brown, "Creeping motion of a sphere through a bingham plastic," *Journal of Fluid Mechanics* **158**, 219 (1985).
- [11] I. C. Walton and S. H. Bittleston, "The axial-flow of a bingham plastic in a narrow eccentric annulus," *Journal of Fluid Mechanics* **222**, 39 (1991).
- [12] N. J. Balmforth and R. V. Craster, "A consistent thin-layer theory for bingham plastics," *Journal of Non-Newtonian Fluid Mechanics* **84**, 65 (1999).
- [13] S. D. R. Wilson, "Squeezing flow of a bingham material," *Journal of Non-Newtonian Fluid Mechanics* **47**, 211 (1993).